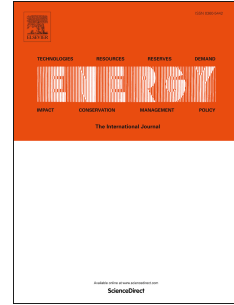


# Journal Pre-proof

Dynamical modelling and experimental validation of a fast and accurate district heating thermo-hydraulic modular simulation tool

A. Dénarié, M. Aprile, M. Motta



PII: S0360-5442(23)01791-7

DOI: <https://doi.org/10.1016/j.energy.2023.128397>

Reference: EGY 128397

To appear in: *Energy*

Received Date: 17 March 2023

Revised Date: 4 July 2023

Accepted Date: 9 July 2023

Please cite this article as: Dénarié A, Aprile M, Motta M, Dynamical modelling and experimental validation of a fast and accurate district heating thermo-hydraulic modular simulation tool, *Energy* (2023), doi: <https://doi.org/10.1016/j.energy.2023.128397>.

This is a PDF file of an article that has undergone enhancements after acceptance, such as the addition of a cover page and metadata, and formatting for readability, but it is not yet the definitive version of record. This version will undergo additional copyediting, typesetting and review before it is published in its final form, but we are providing this version to give early visibility of the article. Please note that, during the production process, errors may be discovered which could affect the content, and all legal disclaimers that apply to the journal pertain.

© 2023 Published by Elsevier Ltd.

## **CRedit authorship contribution statement**

**Alice Dénarié:** Conceptualization, Methodology, Software, Writing – original draft, Writing – review & editing.

**Marcello Aprile:** Conceptualization, Methodology, Software, Writing - Review & Editing.

**Mario Motta:** Supervision, Project administration, Funding acquisition.

Journal Pre-proof

1 **Title**

2 Dynamical modelling and experimental validation of a fast and accurate district heating thermo-hydraulic  
3 modular simulation tool.

4 **Authors**

5 A. Dénarié (<sup>1</sup>), M. Aprile, M. Motta

6 Department of Energy, Politecnico di Milano, 20156 Milano, Italy

7

8 **Highlights**

- 9 • A model for fast and realistic simulation of district heating network is presented  
10 • The heat-transmission pipe is modelled with the method of characteristics with a Lagrangian approach  
11 • An entire big scale district heating model is validated with yearly monitoring data, proving the model  
12 usability  
13 • Simulation results agree with temperatures at distant user's substations and peak demand at generation  
14 plant

---

<sup>1</sup> Corresponding author. Tel.: +39 02 2399 3850; fax: +39 02 2399 3868.

E-mail address: alice.denarie@polimi.it (A. Dénarié).

**15 Abstract**

16 This paper presents a new thermo-hydraulic model for district heating systems simulations, which  
17 aims at being a fast and accurate tool to simulate highly renewable networks characterized by  
18 fluctuating energy profiles. The main novel aspect of the tool lies in the heat transmission modelling  
19 over long pipes based on a Lagrangian numerical approach. In comparison to other existing models,  
20 this approach significantly reduces computational time and it increases results' accuracy. The  
21 elaborated method avoids numerical diffusion in the results and consequently allows proper  
22 prediction of temperature propagation, especially in case of fast changes of fluctuating profiles. The  
23 tool is built following a modular procedural programming approach in order to facilitate the  
24 simulation of multicomponent system. Thanks to its modular structure, every components of the  
25 system is built with the same structure that is differently declined according to each component's  
26 requirements. In this way, new additional elements' models easily fit the existing ones.

27 The model is validated under real operating conditions with hourly monitoring data of an Italian  
28 district heating network.

29 The results show good correspondence also in the most peripheral nodes of the network, where the  
30 largest deviations are normally encountered, thus making the model a reliable and fast simulation tool  
31 for district heating network design and operational control.

**32 Keywords**

33 District heating; modular modelling; dynamic simulation; validation; monitoring data

34

35 **Summary**

36	1	Introduction.....	5
37	1.1	Existing models .....	6
38	1.1.1	Models of the hydraulic problem.....	6
39	1.1.2	Models of the thermal problem .....	7
40	1.1.3	DH systems models .....	8
41	1.2	Motivation of the work .....	9
42	2	Methodology.....	10
43	2.1	The model.....	11
44	2.1.1	The network components' representation.....	12
45	2.1.2	The model structure .....	13
46	2.2	The hydraulic problem.....	14
47	2.3	The thermal problem: two solutions.....	15
48	2.3.1	The lumped capacity method.....	16
49	2.3.2	The characteristics method .....	16
50	3	The case study.....	18
51	3.1	Measurement data.....	19
52	3.2	Simulation results .....	20
53	3.2.1	Substations supply temperature .....	20
54	3.2.2	Return temperature and energy production of generation plant .....	27
55	4	Discussions and conclusions.....	30
56			

57 **Abbreviations**

58 DH District Heating

59 **Nomenclature**60  $a$  friction coefficient,  $\text{m}^{-2} \text{kg}^{-1}$ 61  $C$  linear heat capacity,  $\text{J m}^{-1} \text{K}^{-1}$ 62  $F$  force, N63  $h$  linear heat transfer coefficient,  $\text{W m}^{-1} \text{K}^{-1}$ 64  $L$  pipe length, m65  $m$  mass, kg66  $\dot{m}$  mass flow rate,  $\text{kg s}^{-1}$ 67  $p$  pressure, Pa68  $\dot{Q}$  heat, W69  $T$  temperature,  $^{\circ}\text{C}$ 70  $t$  time, s71  $v$  fluid velocity,  $\text{m s}^{-1}$ 72  $U$  internal energy, W73  $\dot{W}$  work, W74  $x$  pipe section length, m75 **Greek symbols**76  $\theta$  temperature, advection problem solution,  $^{\circ}\text{C}$ 77  $\Delta$  delta, difference78 **Subscripts**79  $B$  equivalent boundary layer (water boundary layer and steel pipe)

80	<i>c</i>	turbulent core
81	<i>diss</i>	dissipation losses
82	<i>e</i>	edge
83	<i>el</i>	electric
84	<i>ext</i>	external environment
85	<i>gen</i>	generation plant
86	<i>i</i>	pipe number
87	<i>in</i>	inlet
88	<i>ins</i>	insulation
89	<i>loss</i>	heat losses
90	<i>n</i>	node
91	<i>out</i>	outlet
92	<i>w</i>	water

## 93 **1 INTRODUCTION**

---

94 District heating systems are energy infrastructures allowing the reduction of primary energy consumption [1]  
95 through the exploitation of local synergies between demand and available sources such as waste heat recovery  
96 and large use of renewable energies [2]. The exploitation of local renewable energy sources, especially in  
97 urban areas where free space is an issue, has brought to several projects of distributed integration of renewables  
98 and waste heat in existing and new DH systems [3–7]. In future energy systems, where heating and electrical  
99 sectors are strongly interconnected through DH, [8] demand side management techniques and flexibility  
100 potentials strategies will be realized in DH systems especially in new generation ones such as 4GDH and  
101 5GDH systems with distributed users located heat pumps [9].

102 Following this trend, DH networks are going to be more complex, with several generation systems distributed  
103 along the network and characterized by highly fluctuating energy profiles. A detailed representation of  
104 temperature fluctuation propagations and pressure drops along these networks is therefore essential for both  
105 planning and operational optimisation. More specifically, it is desirable to evaluate, in each point of the  
106 network and over time, the variables that uniquely describe the status of the system: temperatures, flowrates

107 and pressures. This to better forecast the performances of the distributed generation systems and their impacts  
108 on the network. Despite the well-known governing equations and the existing modelling approaches, the  
109 development of a fast and accurate DH simulation tool capable to predict the thermal and hydraulic behaviour  
110 of a DH network is not a trivial task that still needs further developments. Because of the large extension and  
111 the number of ramifications that usually characterize the DH systems, the effectiveness of thermal networks'  
112 modelling is still an open topic that the work here presented addresses: this paper presents a new thermo-  
113 hydraulic modular simulation model conceived for complex DH systems. The tool novelty lies in the inclusion  
114 of a pipe heat transmission model based on the Lagrangian method of characteristics. The approach, that has  
115 been presented and validated by the authors for one single pipe in [10], is here integrated in a full simulation  
116 tool applied to a big scale DH system. In addition, the tool main advantage is that it' built with a modular  
117 procedural programming approach that facilitates the construction of multiple components models. The  
118 thermo-hydraulic full model accuracy of the entire network is here investigated under real operating conditions  
119 by the comparison with yearly monitoring data of an Italian DH company located in the municipality of Lodi.

## 120 **1.1 EXISTING MODELS**

121 The simulation of DH systems involves the description of both the hydraulic and thermal behaviours. The most  
122 commonly used mathematical model of thermo-hydraulic networks is the pseudo-dynamic [11], which has a  
123 steady-state formulation of the hydraulic problem and a dynamic solution of the thermal one.

### 124 **1.1.1 Models of the hydraulic problem**

125 The first approach to solve flow and pressures propagation over meshed network was developed by Hardy-  
126 Cross and it's based on the independent solution of each network loops by iteration. For a given pipe loop with  
127 known inlet and outlet flowrates, the unknown pipes' flowrates are calculated by an iteration process based on  
128 initially guessed flow values and a corrective factor. Flows' continuity equations at pipe nodes and pressures  
129 drops balances inside the loops are iterated until the corrective factor is zero. The Newton-Raphson method  
130 has been later used to solve water networks problems by applying it to pressure drops function. The method is  
131 matrix based, again iterative, but with multiple corrective factors, one for each flowrate value, and it's based  
132 on linear approximation of pressure drops functions.

133 In [12] the equations describing the hydraulic and dynamic thermal behaviour are solved simultaneously in a  
134 coupled Newton-Raphson power flow calculation. In [13] a new method to solve steady state hydraulics of  
135 complex networks is presented as more efficient and easier than the Hardy Cross method.

136 Some works include hydraulics dynamic behaviours in the modelling such as [14].



137 In [15] a DH model designed for multiple loops network is presented: the hydraulic problem is solved through  
138 the loop equation method, while the thermal one is solved with an upwind finite-difference method.

139 In [16] a method to solve both thermal and hydraulic problems of DH systems involving loops is presented.  
140 The model solves separately the transportation and the distribution networks to reduce computational costs;  
141 mass, momentum and energy conservation equations are written in a matrix form for all networks nodes. A  
142 similar model is applied in [17] to show how to exploit DH flexibility to shave peaks thanks to optimized flow  
143 rate control, while in [18] a model for the optimisation of meshed network is presented.

### 144 **1.1.2 Models of the thermal problem**

145 Several works dealing with the dynamical simulation of temperature propagation along the network have been  
146 found in literature and they are described in the following.

147 Simplifying approaches such as black box models [19] and aggregation methods [20] are useful to reduce  
148 simulation's time; nevertheless they are not adequate to study distributed energy connections in the networks  
149 since the connection with the network topology is lost.

150 Physical models, which explicitly describes the system's physical aspects, are preferred in this work  
151 application [15]. Heat transport physical models can be distinguished according to the method used to solve  
152 the advection problem; two main approaches can be identified: finite element and plug flow. Benonysson  
153 presents these two approaches in [11]: the *element method* is a finite difference method solving energy balance  
154 equations; the *node method* calculates pipes' temperature using time history of inflow temperature and mass  
155 flowrate being a version of plug flow approach.

156 Despite its great accuracy, the element method has two major drawbacks which affects its usability: the  
157 calculation time length and the occurrence of artificial numerical diffusion. Palsson [21] describes a different  
158 discretization scheme to be used in the element method, QUICK, intending to limit the numerical diffusion of  
159 upwind different scheme. Further work on finite difference modelling can be found in [22],[23] where a new  
160 model of pre-insulated twin pipes is presented and in [15] where a model based on finite element is proposed  
161 to simulate networks with multiple meshes.

162 Concerning the node method, its strength is that, based on the plug flow approach, it only calculates incoming  
163 water segment propagation time and thermal losses. In this way, computational efforts are significantly smaller  
164 and artificial diffusion is avoided. The node method tracks the propagation time and the temperature value of  
165 all the water volumes travelling through the pipe. Nevertheless, its drawback can be found in the outlet result  
166 calculation that loses accuracy by mixing outlet volumes temperatures in a single value. Gabrielaitiene has  
167 given major contribution in analysing the node method performances thanks to several studies in comparing it  
168 with other modelling approaches [24], with commercial software TERMIS [25], [26], [27] and with monitoring

169 data [28]. The outcome of these analyses is that the node method is faster and it doesn't show numerical  
170 diffusion, but it presents inaccuracies in distant point of the network with sharp temperature variations. Starting  
171 from the investigations of the node method inaccuracies, the authors of this work have developed a new  
172 Lagrangian numerical approach to simulate heat transmission in DH pipes by solving these issues. The pipe  
173 model presented in [10] is therefore here integrated in a full system model.

174 A similar approach is used in the pipe modelling of TRNSYS software [29]. An implementation of a  
175 Lagrangian approach to deal with the thermal simulation of piping network is presented in [30]: the author  
176 presents a district cooling network model emphasising the success of this modelling approach in particular  
177 with the elimination of numerical diffusion. A more recent paper [31] presents the comparison between the  
178 node method and the full implicit and Crank–Nicolson finite difference approaches: the results aim at helping  
179 future DH optimization tool designers to choose an adequate pipeline model. In [32] a new model approach  
180 combining the features of plug-flow and discrete stirred tank includes the longitudinal dispersion of turbulent  
181 fluid, a novel aspect which is usually neglected, but that gain importance in low flow regime.

182

### 183 **1.1.3 DH systems models**

184 Using the presented approach, DH full system simulation tools have been found in existing works. An  
185 optimisation tool for DH network in [33] uses the pipe model presented in [10] as a planning tool for systems  
186 management. In [16] a full DH model for meshed network is presented based on finite elements approach.

187 In [34] a Lagrangian approach is used in a DH simulation tool: the tool focuses on the solution of the complex  
188 challenges of this numerical approach when a water segment has to traverse a highly branched network using  
189 recursive methods within the timestep. The tool has a particular accuracy in describing the mathematical  
190 approach and is rich in components variety, nevertheless is not validated under real operating conditions.

191 In recent year there has been a growing interest in using object-oriented modelling to simulate DH system. The  
192 plug flow approach has been preferred in this type of application: in [35], Giraud et al. present a Modelica  
193 library conceived to simulate DH networks and solar thermal integration; in [36], Van Der Heijde et al. show  
194 a Modelica software implementation of a thermo-hydraulic plug-flow model for thermal networks and validate  
195 it experimentally.

196 Following the purpose of open source models, some Python [37] based libraries have been built. DHNx [38,39]  
197 is the package inside the Oemof [40] optimisation framework that contains DH network optimization and  
198 simulation models. In [41], DiGriPy, a newly developed Python tool for the simulation of DH networks based  
199 on the TESPpy [42] package is presented.

200 Concerning the use of these models in real operational conditions, there's a general lack of works presenting  
201 validations based on long period measurements of real networks: in [28] the author presents an entire network  
202 validation for 2 winter days, in [27] 4 spring days are considered to validate a DH network, while in [43] a  
203 small DH network is validated during one winter day.

## 204 **1.2 MOTIVATION OF THE WORK**

205 The analysis of existing models presented in the previous section highlights the advantages and limits of the  
206 most commonly used models based on finite element discretization. For these reasons the authors have chosen  
207 to developed a thermo-hydraulic model, which is here presented and investigated in its accuracy, with a novel  
208 modelling approach depending on the spatial extension of the system components.

209 The main strength of the work here described is represented by the modularity of the simulation tool, able to  
210 model complex system and flexible enough to choose the appropriate modelling approach for each component  
211 with the ambition to pursue a good compromise between simulation's accuracy and rapidity. The modular  
212 procedural programming approach used in the coding phase is particularly suitable for the modelling of  
213 multicomponent phase system. In fact, this programming syntax keeps the same common modelling  
214 framework for all the elements but it allows every component to be described by its own characteristic  
215 equations solved with different approaches.

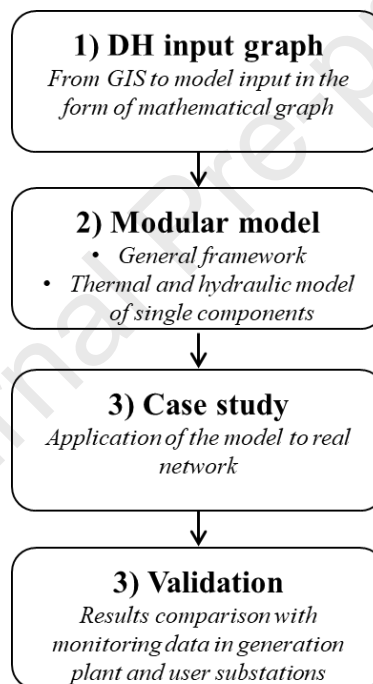
216 The flexibility of the instrument is best expressed in the choice of the approaches to solve the thermal problem,  
217 different for each component. For all components that do not have a prevailing geometric dimension, a lumped  
218 capacity approach is used where the spatial discretization coincides with the single element. For the network  
219 pipes' model, the variable spatial discretization defined by the method of characteristics is chosen as presented  
220 by the author in [10]. In [10], the turbulent flow heat transmission model has been tested in a single pipe  
221 application: the results have shown that the temperature profile over long pipes is properly reproduced. Still,  
222 the benefits of this modelling approach can be fully appreciated only at the entire system scale, especially big  
223 scale system, which is instead shown in this paper. The aim of this paper is to show that the promising results  
224 presented in [10] for a single pipe are confirmed along the entire network together with the hydraulic behaviour  
225 prediction. The validation through the entire network modelling is particularly important in the Lagrangian  
226 approach because, differently from existing models, it allows the water volumes tracking though the entire  
227 network, in junctions and mixing points. The full model here presented allows fast simulations of big scale  
228 system with high quality accuracy especially in peripheral network points in case of rapid temperature  
229 variations.

230 After recalling the main assumptions and equations constituting the thermal and hydraulic models, the paper  
 231 presents the comparison between the temperatures predicted by different simulations and their experimental  
 232 counterparts.

233

## 234 2 METHODOLOGY

235 The aim of this work is to present the developed model and to validate its accuracy by applying it to a real DH  
 236 network to simulate its behaviour. The main methodological steps are shown in Figure 2.1 and described in  
 237 the following.



238

239

Figure 2.1 Methodological steps

240 First the geometry of the DH system, the network in particular, is taken from a GIS (Geographical Information  
 241 System) file and converted in a mathematical graph as described in paragraph 2.1.1. The network graph is the  
 242 input of the second step, the dynamical model, that is described in detailed in this chapter. The general modular  
 243 modelling framework is developed and declined to every component's model to solve the hydraulic and  
 244 thermal problem, solved in parallel, as described in 2.1.2, 2.2 and 2.3. The two available approaches to solve  
 245 the thermal model, the lumped capacity upwind discretization and Lagrangian characteristics method, are  
 246 described in 2.3. The Lagrangian approach implemented in this model can be used for tree shaped network

247 only, for meshed network the lumped capacity upwind scheme is used. The model is written in Matlab and can  
 248 be used to simulate city scale DH system with several users (in this case almost hundreds).

249 The built model is then applied to a real network in the north of Italy where a reference year has been used to  
 250 simulate the hourly behaviour of the entire system. Finally the results of the simulations are compared to  
 251 monitoring data in the main generation system, paragraph 3.2.2 and in user substations 3.2.1.

## 252 **2.1 THE MODEL**

253 This section describes the structure of the simulation tool and the mathematical model built to simulate pressure  
 254 drops and temperature transient along the network. The main purpose of this modular simulation tool is the  
 255 solution of the thermal and hydraulic problems characterizing the overall DH system that is here represented  
 256 by a graph with edges and nodes. Each element's thermal and hydraulic behaviour is modelled through the  
 257 equations of mass, momentum and energy conservation, declined differently for each component. The obtained  
 258 outputs are the independent variables describing the system behaviour, in time  $t$  and space  $x$  in each  $i$  node of  
 259 the network:

- 260 • Temperature  $T_i(x, t)$
- 261 • Pressure  $p_i(x, t)$
- 262 • Mass flowrate  $\dot{m}_i(x, t)$

263 The network is mathematically represented by a graph whose edges are the components constituting the system  
 264 and the nodes represent the joints where the balance equations occur.

265 The model is based onto the following hypothesis:

- 266 • the water is considered as an incompressible and homogenous fluid;
- 267 • the material properties have constant values;
- 268 • the timestep is constant;
- 269 • the Lagrangian approach is used for pipes in tree shape network while finite difference is used for  
 270 meshed network.

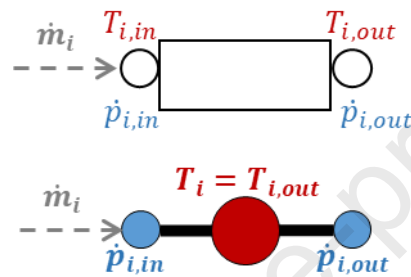
271 The model currently includes the following elements models that are described in detail in the Appendix:

- 272 • Pipe: main element of the distribution network that generates heat losses and pressure drops.
- 273 • Pump: element that increases the pressure in the system and covers the friction losses thanks to  
 274 electrical consumption. Two types are available fixed and variable speed. It usually represents the  
 275 main pumping sites in the central plant.
- 276 • Generation plant: heat producer with a certain efficiency responsible for keeping a certain set point of  
 277 supply temperature.

- 278 • User substation: heat exchanger that represents the heat consumption at customers' substation causing  
 279 a temperature reduction and pressure drop between supply and return line.

### 280 2.1.1 The network components' representation

281 The system is mathematically built as a graph where the components are modelled as edges connected by  
 282 initial and final nodes. Every element has one lumped capacitance thermal node and two zero-capacity  
 283 hydraulic nodes, characterized by their relative variables, temperature  $T_i$  and pressures  $p_i$ , as shown in Figure  
 284 2.2.



285  
 286 *Figure 2.2 Scheme of equivalent edge model: two blue hydraulic nodes and one single red thermal node*

287 The temperature of the edge is assimilated by its outlet node temperature. Every system's component is  
 288 modelled by its constitutive equations: a unique modelling structure is however kept common for all the  
 289 components to facilitate elements' connections following a procedural programming approach.

290 The network geometry input is built from the network GIS (Geographical Information System) shape file that  
 291 is processed with a sequence of steps that connects edges and nodes and identify common nodes between  
 292 edges. In particular, the application of the Depth-First Search algorithm [44], one of the most common graph  
 293 algorithm, allows the subsequent numbering from the root point - the generation plant - towards the most  
 294 peripheral points of the tree graph - the users. In this model, the supply and return line are symmetrical so the  
 295 path is done backward for the return line. Figure 2.3 shows the resulting numbering of the system elements.  
 296 This ordered graph representation of the network is of particular importance since the solution of the  
 297 distribution network heat propagation model is performed with a Lagrangian approach, so the order of the  
 298 elements solution has an impact on the calculation.

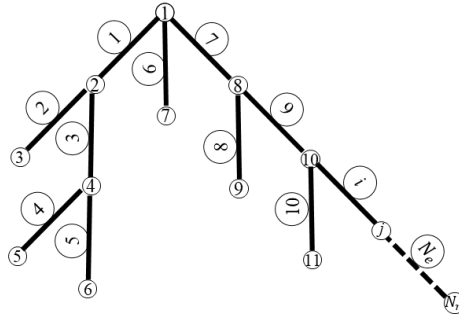


Figure 2.3 Exemplification of the numbering of DFS algorithm

299

300

301 The mathematical description of the entire system is therefore a graph composed by  $N_n$  nodes and  $N_e$  edges,  
 302 where the edges are constituted by the network elements, such as pipes, pumps, heat exchangers, generation  
 303 plant etc.; the nodes represent the points that connect the edges.

304 Two main structures are generated to contain all the information of system's geometry in order to solve the  
 305 thermal and hydraulic network: the *edge-node* matrix and the *node-path* function. The *edge-node*  $N_e \times N_n$   
 306 matrix contains 1, -1 or 0 if an edge flow is entering or leaving a node or it is not connected [16].

307 The *node-path* function, built applying the Dijkstra's Shortest Path Algorithm between the node and the  
 308 root node, describes, for every node, the sequence of all nodes crossed in the path to the generation plant. This  
 309 function therefore creates the sequence of flow propagation from the generation plant to users' substations and  
 310 back [15]. The flow propagation order defines therefore the elements simulation sequence of the thermal  
 311 problem.

### 312 2.1.2 The model structure

313 A pseudo-dynamic solution method is used in this tool since the hydraulic problem is solved as steady state –  
 314 hydraulic nodes has no capacitance- while the thermal problem includes capacities and therefore dynamics.  
 315 The appendix describes the detailed equations for every elements model.

316 Figure 2.4 summarises the main steps performed in the modelling tool to solve the entire system simulation  
 317 that are afterwards detailed in the Appendix.

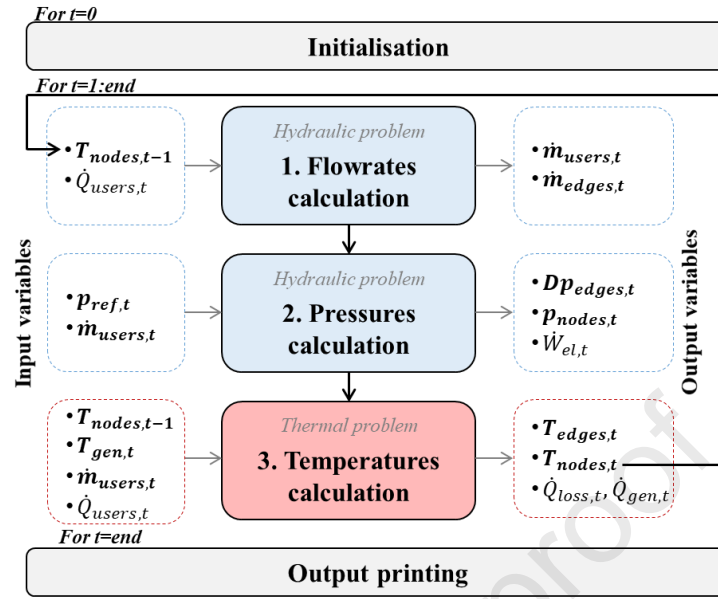


Figure 2.4 Structure of model solution's steps

318

319

320 In each simulation time step, the hydraulic problem is solved with a steady-state approach, starting from the  
 321 calculation of the flow rates  $\dot{m}_{user,t}$  required at current timestep  $t$  at users' substations. In this step all  
 322 flowrates  $\dot{m}_i$  and pressures  $p_j$  of all edges  $i$  and nodes  $j$  are calculated along the network with the use of the  
 323 *edge-node* matrix as described in section 2.1.1. Substations flowrates are determined with the customers  
 324 required heat  $\dot{Q}_{user,t}$  and with the supply temperatures to the heat exchangers  $T_{nodes,t-1}$ , being the latter  
 325 calculated from the solution of the thermodynamic problem at the previous timestep. Within the time step  
 326 when the thermal problem is solved, the flow rates are assumed to be constant. Thanks to the known flowrates  
 327 in all the edges, the propagation of the input temperature from the generation plant  $T_{gen,t}$  is calculated along  
 328 the supply line of the network. Similarly, in the return line, the temperature profiles coming for the return  
 329 temperature at user substations is propagated to the generation plant. The temperatures in all the points of the  
 330 network  $T_{edge,t}$  and  $T_{node,t}$  are therefore calculated at the new timestep  $t$  in a dynamic way so including also  
 331 previous timestep values as described in section 2.1.1. The new obtained temperature distribution allows the  
 332 flow rates calculation in the following time step. An unavoidable time-lag of one-time step, due to the  
 333 calculation method, is therefore maintained in the simulation. The appendix shows the details of the procedural  
 334 approach used in every modelling step and the variables calculation.

## 335 2.2 THE HYDRAULIC PROBLEM

336 Pressures and flows' calculation is based on the mass and momentum continuity equation.



337 The mass conservation equation ( 2.1) is applied at every node to calculate the flowrate distribution along the  
 338 network.

$$\sum_i m_i = 0 \quad (2.1)$$

339 The known terms are represented by the flowrate required at user substations which are usually known from  
 340 monitoring results or calculated from users' consumptions. The inlet and outlet flows at every node are  
 341 identified by the *edge-node* matrix. Once the flowrates are obtained, the steady state momentum balance  
 342 equation is applied to all  $N_e$  edges to calculate pressure drops in pipes.

$$\frac{\partial p_i}{\partial x} + F_{fi} = 0 \quad (2.2)$$

343 Using the pipe length as spatial discretization in equation ( 2.2), the pressure drops can be calculated as:

$$\Delta p_i = -a_i L_i \dot{m}_i^2 \quad (2.3)$$

344 Where  $a_i$  is the friction coefficient and  $L_i$  is the pipe length. The  $N_e$  equations ( 2.3) give the pressure  
 345 distribution in the entire network from the pumping systems to the expansion vessel. The expansion vessel is  
 346 considered as the reference node of the hydraulic circuit with an assigned pressure value.

347 In case of tree structured network, the system with  $N_n$  equations of mass continuity on nodes is determined. In  
 348 case of meshed network with closed loop, the system is not determined. It is therefore necessary to add one  
 349 additional equation for every mesh to obtain the mass flowing inside the loop: the sum of pressure drops inside  
 350 the mesh should be equal to zero. To solve these additional equations, the Hardy Cross method has been used  
 351 in this work.

### 352 **2.3 THE THERMAL PROBLEM: TWO SOLUTIONS**

353 The equation governing the problem is the conservation equation of energy ( 2.4):

$$\rho_i A_i c_{p,i} \frac{\partial T_i}{\partial t} + \rho_i A_i v_i c_{p,i} \frac{\partial T_i}{\partial x} + A_i v_i \frac{\partial p_i}{\partial x} + \dot{Q}_i + \dot{W}_i = 0 \quad (2.4)$$

354 The equation represents the energy balance over the cross sectional area, so expressed in a linear form: the rate  
 355 of change of the energy stored in the water section  $A$  is equal to the flux of enthalpy crossing the element and  
 356 the heat  $\dot{Q}$  and the electrical work  $\dot{W}$  entering the element. (e.g. heat supplied by the generator in the boiler  
 357 model, electrical input in the pump model, etc.). The solution of the energy balance equation in the thermal  
 358 problem allows obtaining the variable  $T_i(x, t)$ . Two numerical approaches are here used to solve the thermal  
 359 problem: the lumped capacity method for punctual elements and the method of characteristics for pipes. The

360 “punctual” components are the ones for which parameters describing them do not change over the longitudinal  
 361 direction such as pumps, heat exchangers and generation systems.

### 362 2.3.1 The lumped capacity method

363 According to the lumped capacity method, the elements are modelled as a single node with the entire capacity  
 364 concentrated in one single point and uniform temperature. The hypothesis of temperature uniformity allows  
 365 substituting the temperature spatial derivative with the temperature difference between input and output in the  
 366 energy balance. Using an upwind discretization scheme, all the capacity is lumped at the outlet section of the  
 367 element. In this way, the element  $i$  temperature difference between inlet and outlet becomes the temperature  
 368 difference between element  $i$  and the previous  $i-1$ .

$$\frac{dT_i}{dx} = \frac{(T_{i,in} - T_{i,out})}{\Delta x} = \frac{(T_{i-1} - T_i)}{L_i} \quad (2.5)$$

369 Consequently, for elements' thermal node, equation ( 2.4) becomes:

$$\rho_i A_i c_{p,i} \frac{\partial T_i}{\partial t} = \dot{m}_i c_{p,i} \frac{(T_{i-1} - T_i)}{L_i} + A_i v_i \frac{(p_{i-1} - p_i)}{L_i} + Q_i + W_i \quad (2.6)$$

370

### 371 2.3.2 The characteristics method

372 The heat transmission over distribution pipes has been modelled with a new numerical approach [10] based on  
 373 characteristics method [45]. The detailed description of the method can be found in [10] and it is here  
 374 summarized. The model includes also the turbulent flow characteristics therefore the energy balance equation  
 375 applied to the pipe is split between the water core and the boundary steel pipe including the boundary water  
 376 layer. The energy balance equation ( 2.4) applied to the network pipes is split in the system ( 2.7):

$$\begin{cases} \frac{\partial T_w}{\partial t} + v \frac{\partial T_w}{\partial x} + \frac{h_B}{C_w} (T_w - T_B) = 0 \\ \frac{\partial T_B}{\partial t} + \frac{h_B}{C_B} (T_B - T_w) + \frac{h_{ins}}{C_B} (T_B - T_{ext}) = 0 \end{cases} \quad (2.7)$$

377 The first equation is the energy balance for turbulent water core; the second is for a boundary layer including  
 378 water viscous and diffusive layer and the steel pipe, as Figure 2.5 shows. The thickness of the sublayer and its  
 379 linear heat transfer  $h$  are calculated according to Gnielinski formulation [46].

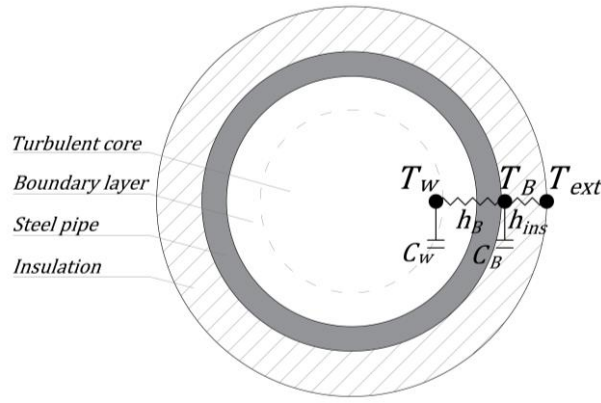


Figure 2.5 Two nodes model of heat transmission in water pipe

380

381

382 The mathematical approach used to solve the system is the splitting approach [47] which consists in splitting  
 383 the system in the advection problem ( 2.8) and the source problem ( 2.10)

$$\begin{cases} \frac{\partial \theta_w}{\partial t} + v \frac{\partial \theta_w}{\partial x} = 0 \\ \theta_w(x, t_0) = T_{w0}(x) \end{cases} \quad (2.8)$$

384 The advection problem is solved with characteristics method for which

$$\theta_w = T_w(x_0) = T_w(x - v \Delta t) \quad (2.9)$$

385 Boundary layer' thermal capacity and heat losses effects are accounted for by solving the source problem:

$$\begin{bmatrix} \frac{dT_w}{dt} \\ \frac{dT_B}{dt} \end{bmatrix} = \begin{bmatrix} -\frac{h_B}{C_w} & \frac{h_B}{C_w} \\ \frac{h_B}{C_B} & -\frac{h_B + h_{ins}}{C_B} \end{bmatrix} \begin{bmatrix} T_w \\ T_B \end{bmatrix} + \begin{bmatrix} 0 \\ \frac{h_{ins}}{C_B} T_{ext} \end{bmatrix} \quad (2.10)$$

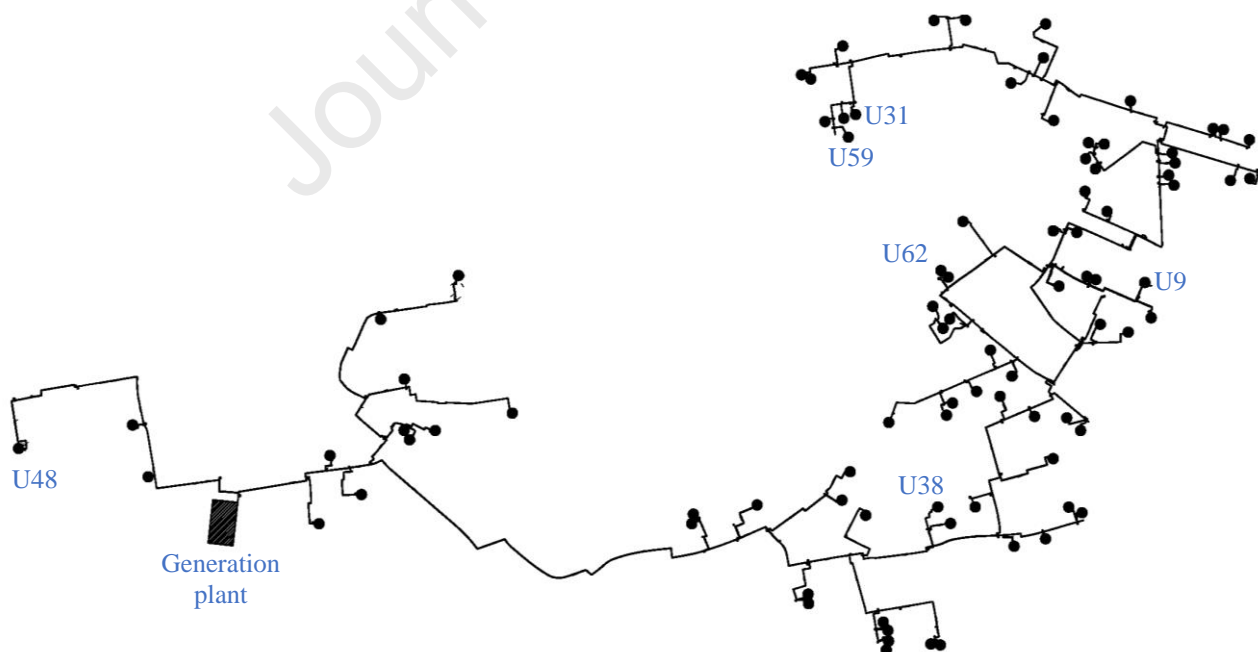
$$T_w(x, 0) = \theta_w(x, t)$$

$$T_B(x, 0) = \theta_B(x, t)$$

386 Where  $T_w$  is the temperature of the water turbulent core and  $T_B$  is the temperature of the boundary layer. The  
 387 system is analytically solved by being in the form of ordinary differential equation  $\frac{dT}{dt} = [A] T + b$ . Following  
 388 the Lagrangian approach, the solution order of pipes' equations is defined by the *node-path* function presented  
 389 in 2.1.1.

### 390 3 THE CASE STUDY

391 The installation of Lodi district heating dates to 2004 and, at the end of 2012, 90 users were connected,  
 392 corresponding to 1 267 600 m<sup>3</sup> of building volumes (approximately 10 000 inhabitants). Out of this volume,  
 393 560 600 m<sup>3</sup> is the share of residential buildings while 707 000 m<sup>3</sup> represents administrative, commercial and  
 394 tertiary users. The generation park consists of a natural gas cogeneration plant with a capacity of 3.86 MW<sub>el</sub>  
 395 and 3.83 MW<sub>th</sub> and 29 MW<sub>th</sub> of natural gas back up boilers. The renewable share of thermal production is  
 396 given by the heat recovery from a third party biomass ORC [48]. An important extension project has started  
 397 in 2014 which implies approximately 30 new substations per year till the end of 2018, reaching 200 users. In  
 398 this work the system is analysed in the configuration of 2013 before the extension. DH provides 36.7 GWh of  
 399 heat, of which the 16% is represented by heat losses. The heating season lasts from mid-October to mid-April.  
 400 During summer, the system delivers heat only to produce domestic hot water which represents the 14% of the  
 401 total heat production over the year. DH consumers to whom heat is delivered heat for DHW production usually  
 402 have centralized distribution system with storage tanks, instead of producing DHW instantaneously; this leads  
 403 to a quite flat load profile for DH systems in summer time. The winter months, on the contrary, are  
 404 characterized by a much more variable profile: space heating systems are generally radiators which are  
 405 regulated with night set-back and intermittent operation during the day. This leads to a fluctuating demand  
 406 profile with pronounced peaks.



407  
 408 *Figure 3.1 Lodi district heating system network in 2013.*

409 A 600 m<sup>3</sup> storage tank helps reducing peak demands at the generation plant and it allows a better management  
 410 of the generation systems. Figure 3.1 shows the district heating system: the distribution network is 15 km long  
 411 and it is made of pre-insulated pipes ranging in diameter from 32 to 300 mm.

412 Consumers are connected through flat plate heat exchangers: the primary side of the substation is regulated by  
 413 a control system which reacts to consumer behaviour to guarantee temperature set points on the secondary  
 414 side.

415 The main effect of user energy demand is a variation in flow rate and return temperature on the substation; on  
 416 the heat generation side, the DH supply temperature is set in order to supply enough energy to all consumers.

### 417 3.1 MEASUREMENT DATA

418 Monitoring data used in this study includes temperatures, flowrates and energy delivered on the primary side  
 419 of users' substations as well as supply temperature from the generation plant. Data were collected with 1-hour  
 420 time step along the year by the remote data logging systems installed on the substations. The generation plant  
 421 data logger instead records data every four days a week in the heating season, from October to March. The  
 422 uncertainties related to measurement tools are shown in Table 3.1

Position	Measure	Tool	Error	Unit
Substation	Flow rate	Ultrasonic flowmeter	$\pm(2 + 0.02 \cdot \frac{\dot{m}_{nominal}}{\dot{m}})$	%
Substation	Temperature	Pt 500	$\pm(0.5 + 3 \cdot \frac{\Delta T_{min}}{\Delta T})$	%
Central plant	Flow rate	Magnetic flowmeter	$\pm(0.5 \cdot \dot{m})$	%
Central plant	Temperature	Pt 500	$\pm(0.3 + 0.005 \cdot T)$	[°C]

423 *Table 3.1 Uncertainty of measurement data*

424 Simulations' results have been analysed to validate the model ability to properly predicts network dynamics.  
 425 The comparison between model outcomes and monitoring data has been done at the inlet of users' substations,  
 426 to check supply temperatures to consumers, and at the generation plant, to check the overall network return  
 427 temperature. Particular attention has been given to this last value and to peripheral users' supply temperatures  
 428 since the main outcome from previous studies about existing models [26] is that the discrepancies between the  
 429 predicted and measured temperatures are bigger for distant consumers.

430 For winter regime, five days of December (9<sup>th</sup> to 14<sup>th</sup>) have been analysed, while for mid-season regime, with  
 431 low space heat demand, the last days of October (21<sup>st</sup> to 28<sup>th</sup>) have been considered.

432 For yearly performances validation, the simulated total heat production and heat losses are compared with  
 433 monitoring data given by the DH company.

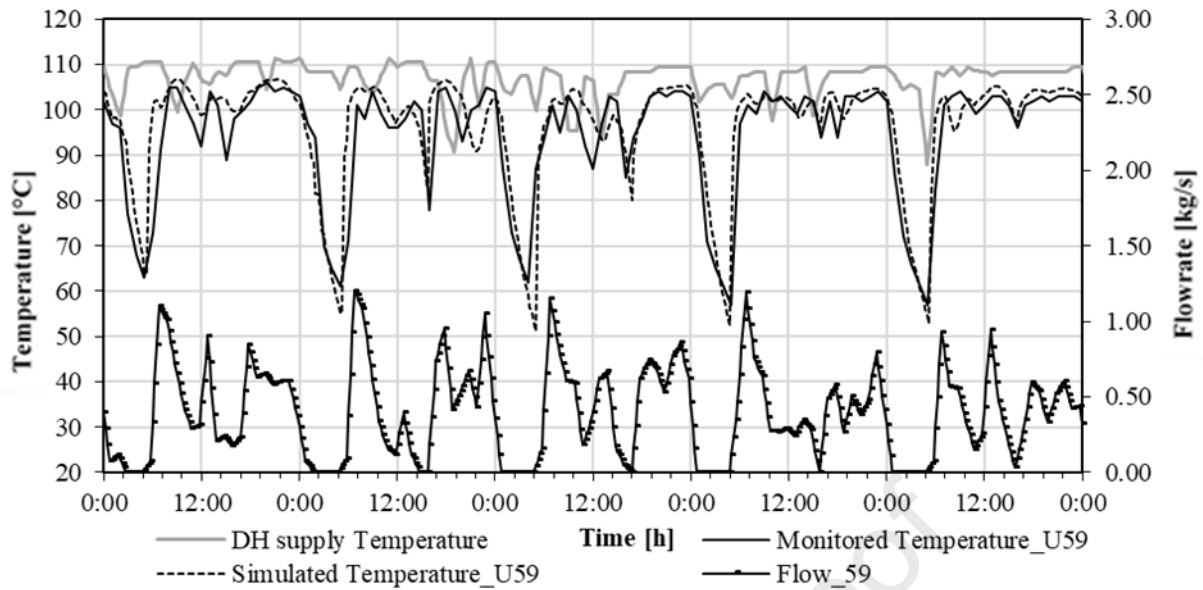
## 434 **3.2 SIMULATION RESULTS**

435 In this section the results of the dynamic simulation of the entire system are presented and compared to  
436 monitoring data in order to validate the model. Specific attention is given to the temperature propagation in  
437 the network in terms of the value of the temperature but also of the timely profile. To do this, the variables  
438 requiring specific analysis are the simulated temperatures at the furthest points from the input data: namely the  
439 supply temperatures at the users' substations to verify the propagation on the supply line and the return  
440 temperature at the main generation plant to verify the results on the return line.

441 With regard to the first point, the average error and the mean square deviation of the supply temperatures at  
442 the users' substations are presented in 3.2.1. First some significant substations, marked on the map of Figure  
443 2.1, are analysed in detail and then the error trend of all substations is reported in Figure 3.12 in relation to  
444 their distance from the central plant station. This aspect in particular is emphasised since one of the literature  
445 review outcome is that the simulation error increase with the distance from the input point. The aim here is to  
446 show that the developed model neither amplifies nor propagates the error along the network. In a specular way,  
447 the propagation of the error on the return line is shown to be avoided by verifying the simulation result with  
448 the monitoring of the network return temperature at the generation plant in paragraph 3.2.2. The overall DH  
449 system simulation results in terms of energy, e.g. annual production, heat losses and electrical consumptions  
450 for the circulation pumps, are finally illustrated in comparison with the monitoring data in paragraph 3.2.2 to  
451 validate the overall model of the entire system in terms of consumptions.

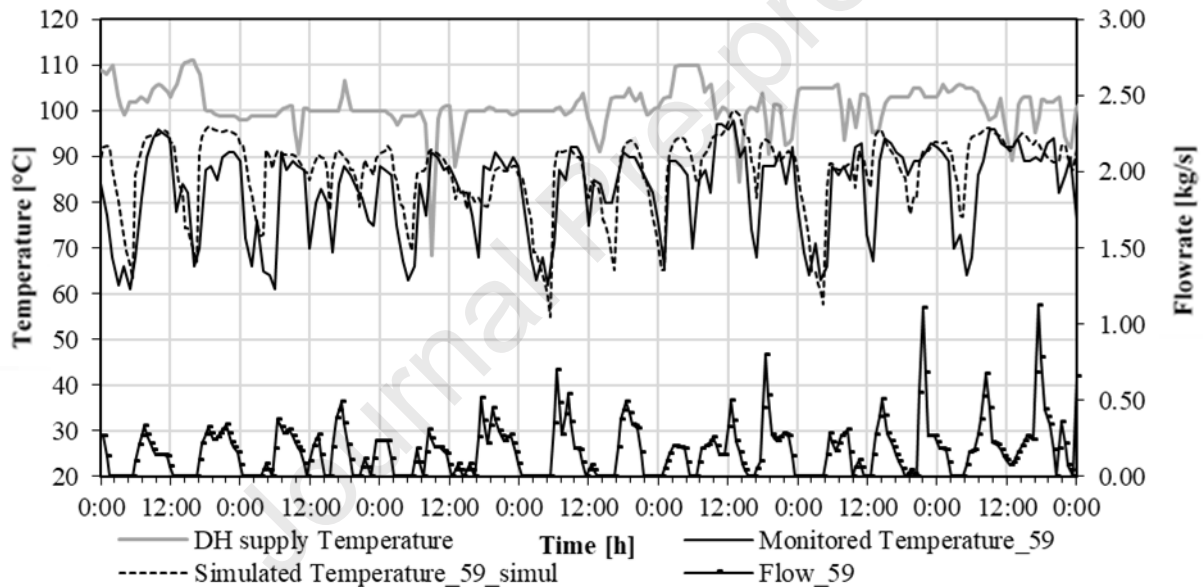
### 452 **3.2.1 Substations supply temperature**

453 Supply temperatures at user substations are here presented comparing simulation results to monitoring data.  
454 Figure 3.1 shows the analysed users: they are located in peripheral nodes of the network, they have different  
455 load profiles and they serve buildings with different use. They have been chosen to test the model validity with  
456 respect to temperature propagation along the network with fluctuating water flows and input temperatures.  
457 Figure 3.2-Figure 3.11 show the results from the selected users and Table 3.2 summarizes the differences  
458 between modelled and monitored temperatures as a function of the distance from the generation plant.



459  
460

Figure 3.2 Supply temperature and flow rate for user 59 – residential - December

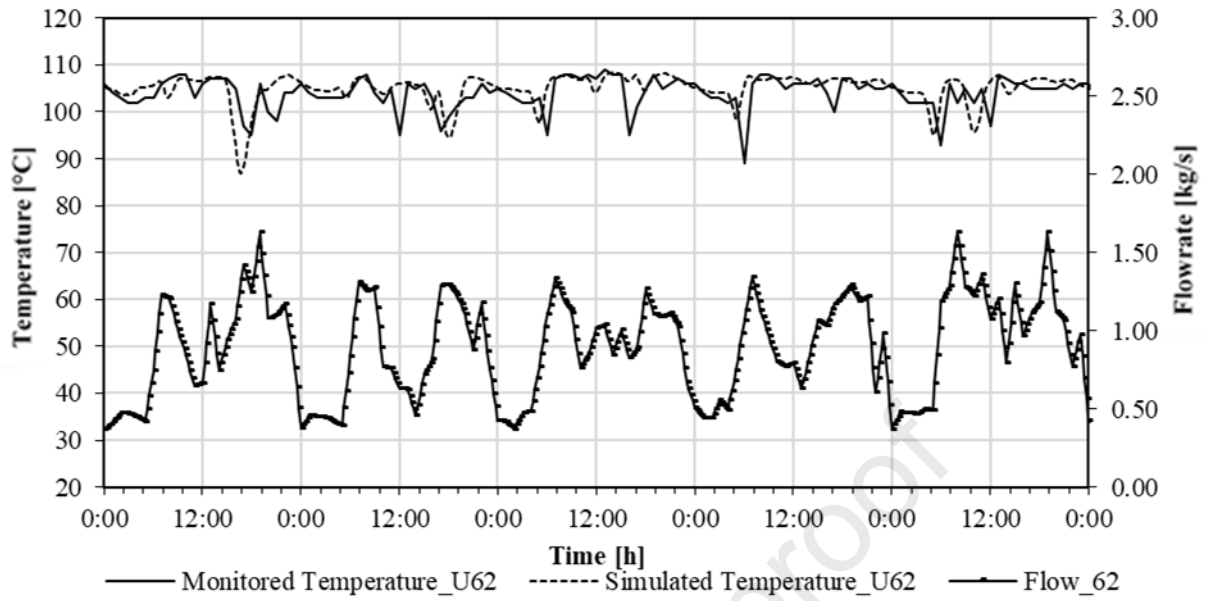


461  
462

Figure 3.3 Supply temperature and flow rate for user 59 – residential - October

463 Looking at simulations outputs, it can be noticed that the model results are in substantial agreement with  
 464 monitored data for all load types and without particular influence of the substation distance on the deviations.  
 465 User 59 is a residential building with the typical flow profile characterizing residential heat demand in Italy.  
 466 Night setbacks with the consequent important morning peaks demand clearly stand out from Figure 3.2. The  
 467 model proves to satisfactorily simulate the temperature propagation as well as the evening temperature drop  
 468 and the fast and wide increase after the morning switch on. It's worth noticing that user 59 is the most distant  
 469 from the generation plant: temperature wave has not been smoothed and transmission time is respected.

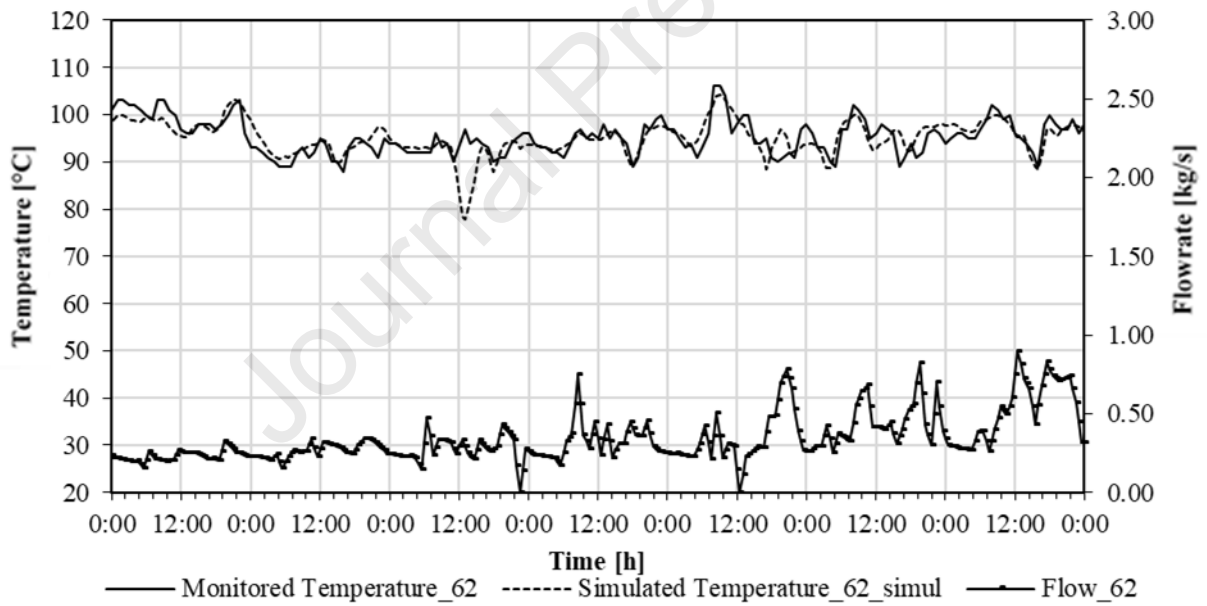




470

471

Figure 3.4 Supply temperature and flow rate for user 62 – residential – December



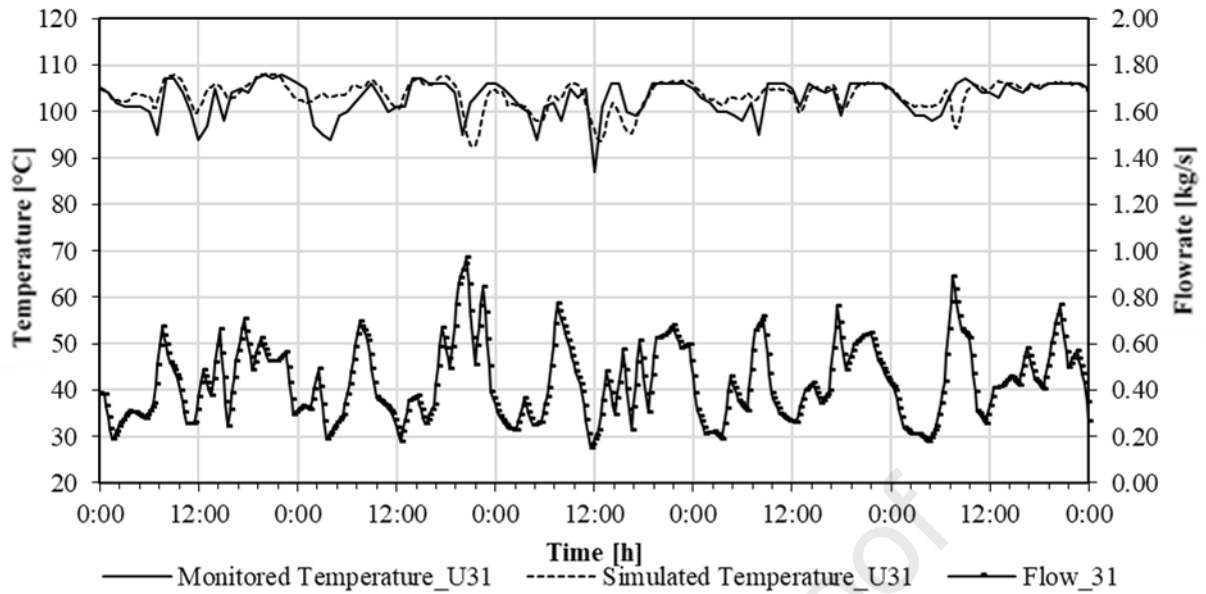
472

473

474

Figure 3.5 Supply temperature and flow rate for user 62 - residential - October

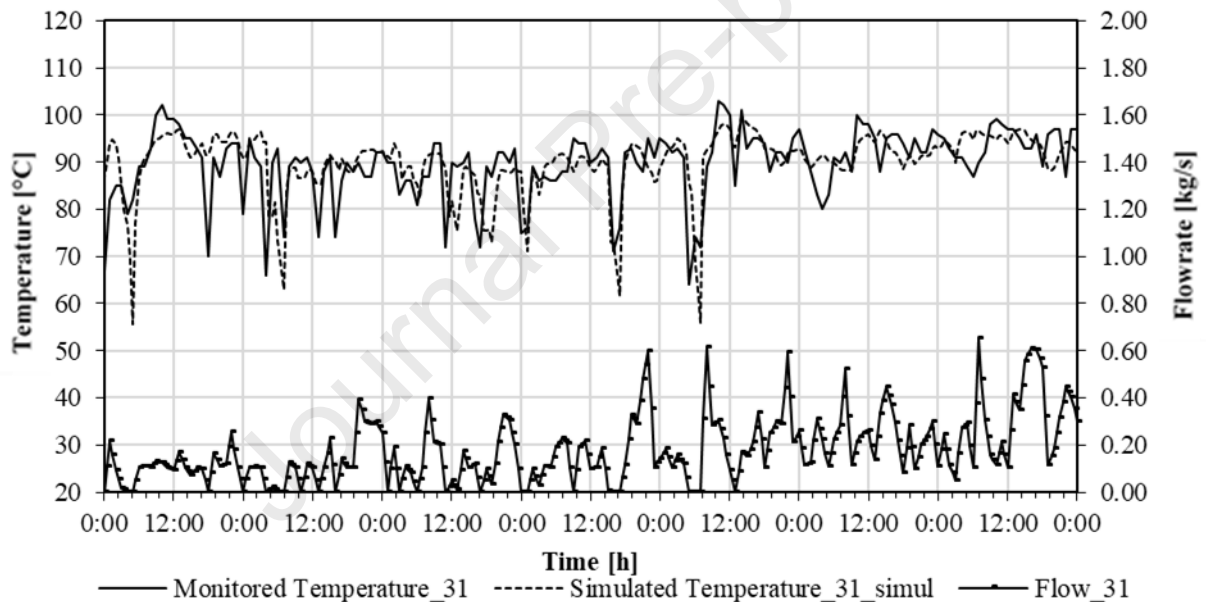




475

476

Figure 3.6 Supply temperature and flow rate for user 31 – residential - December



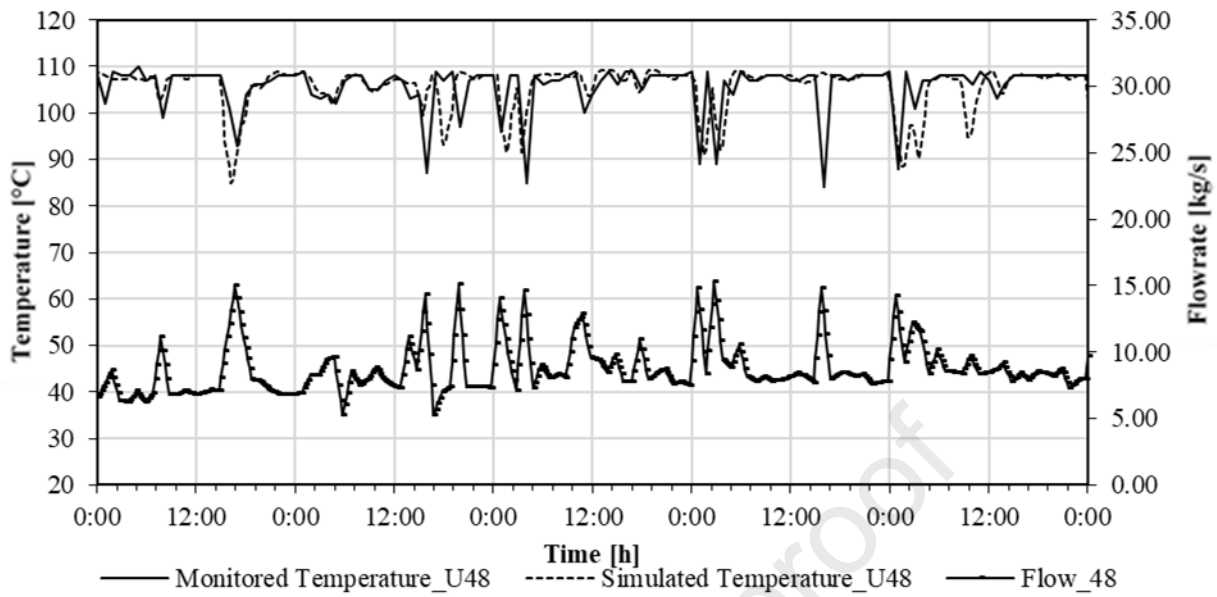
477

478

Figure 3.7 Supply temperature and flow rate for user 31 – residential - October

479 Consumers 62 and 31 (Figure 3.4-Figure 3.5 and Figure 3.6-Figure 3.7) have a quite irregular load demand  
 480 with important fluctuations during the day, with no night set back.

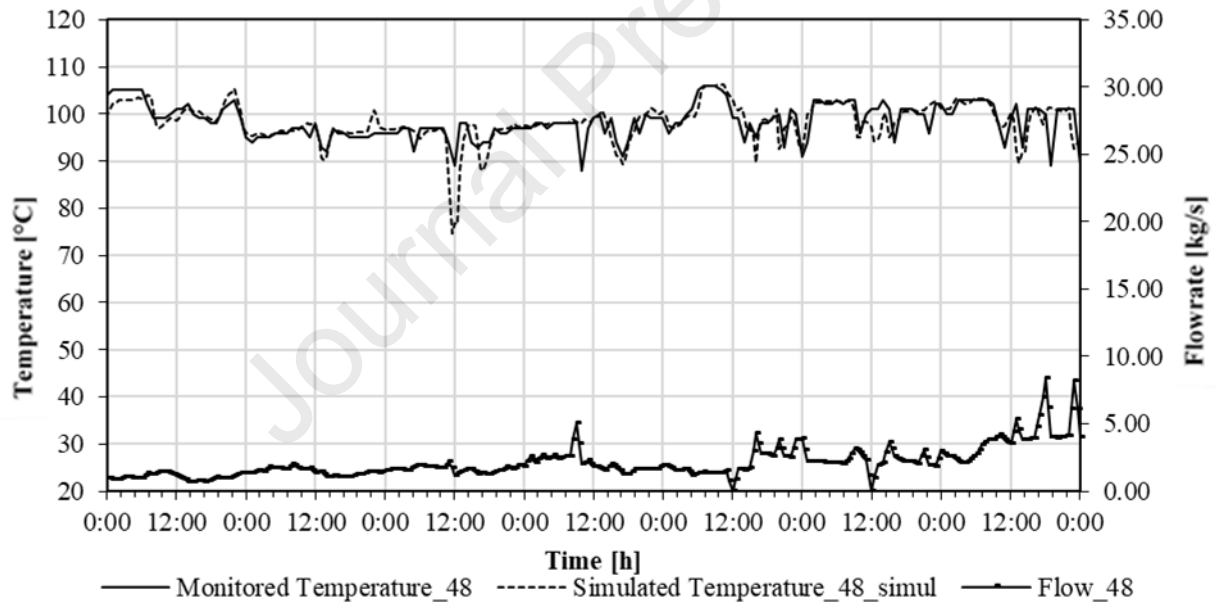
481 Consumer 31 is located close to 59 so in the most peripheral area of the DH system; user 62 is located in the  
 482 area of the system in which the network is meshed. The validation of the model in this point allows validation  
 483 of the hydraulic solution of the meshed network.



484

485

Figure 3.8 Supply temperature and flow rate for user 48 – educational - December



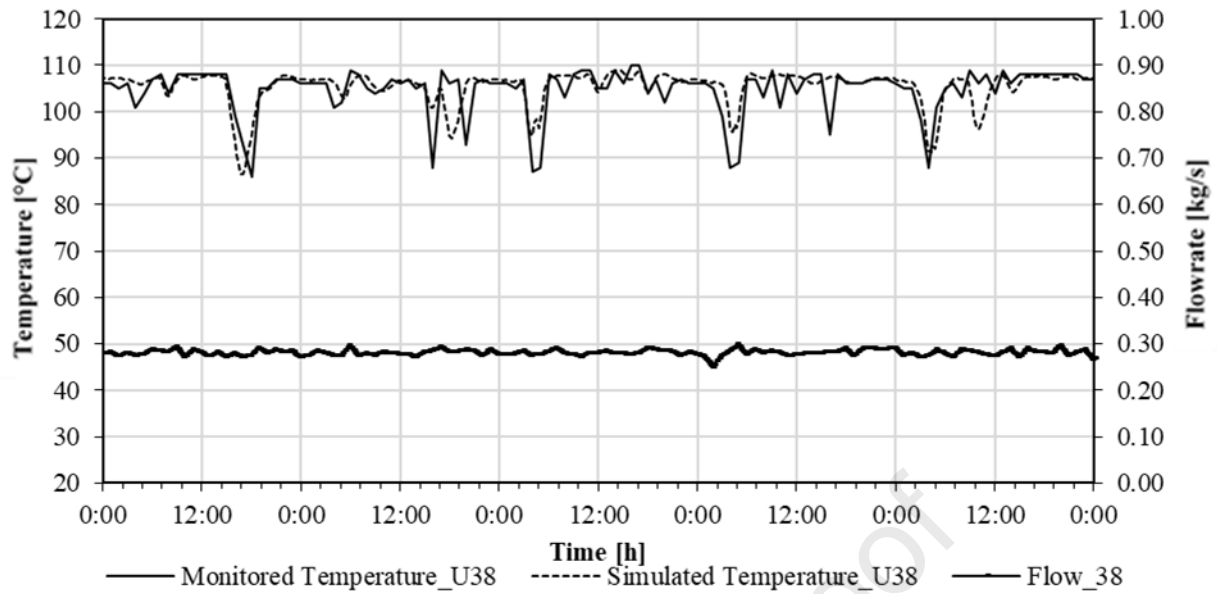
486

487

Figure 3.9 Supply temperature and flow rate for user 48 – educational - October

488 User 48 is the last consumer on the left branch of the network and it's also the biggest user with an annual heat  
 489 load corresponding to 11% of the total DH heat demand. Finally, Figure 3.10 and Figure 3.11 show results for  
 490 consumer 38: this user has an almost constant flowrate which allows validating the propagation phenomena  
 491 from generation plant alone without the influence of user dynamics.

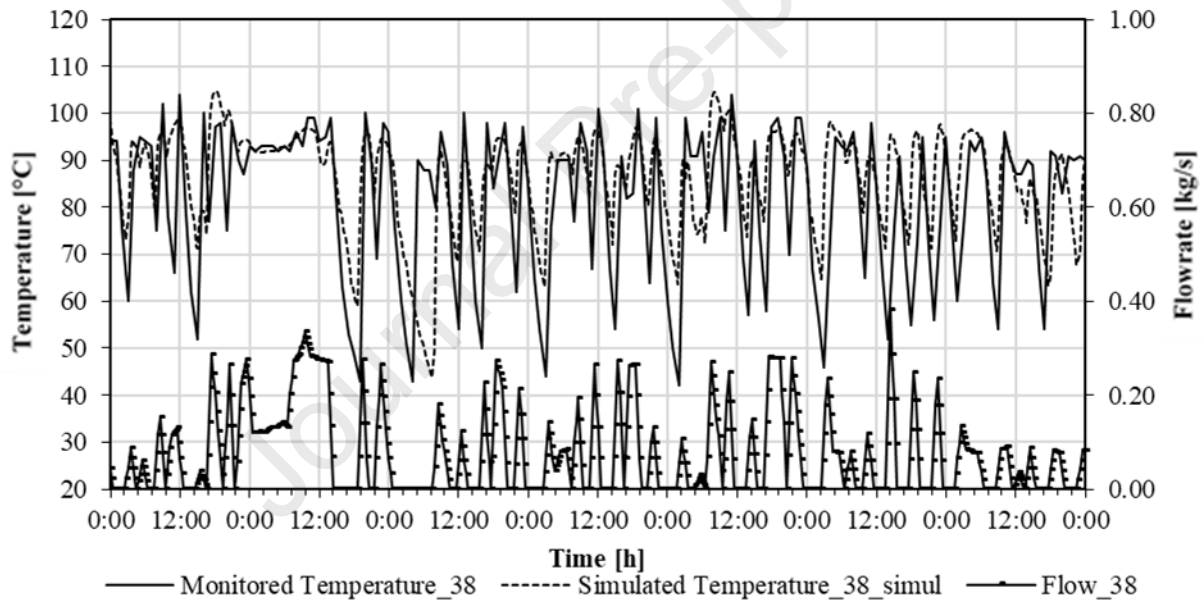
492



493

494

Figure 3.10 Supply temperature and flow rate for user 38 – health - December



495

496

Figure 3.11 Supply temperature and flow rate for user 38 - health - October

497 Table 3.2 summarizes supply temperature's average errors and their standard deviations for all the presented  
 498 users. The table includes also the users' distance from generation plant. No particular correlation between the  
 499 error and the user location can be observed: neither on the average error, neither on its standard deviation.

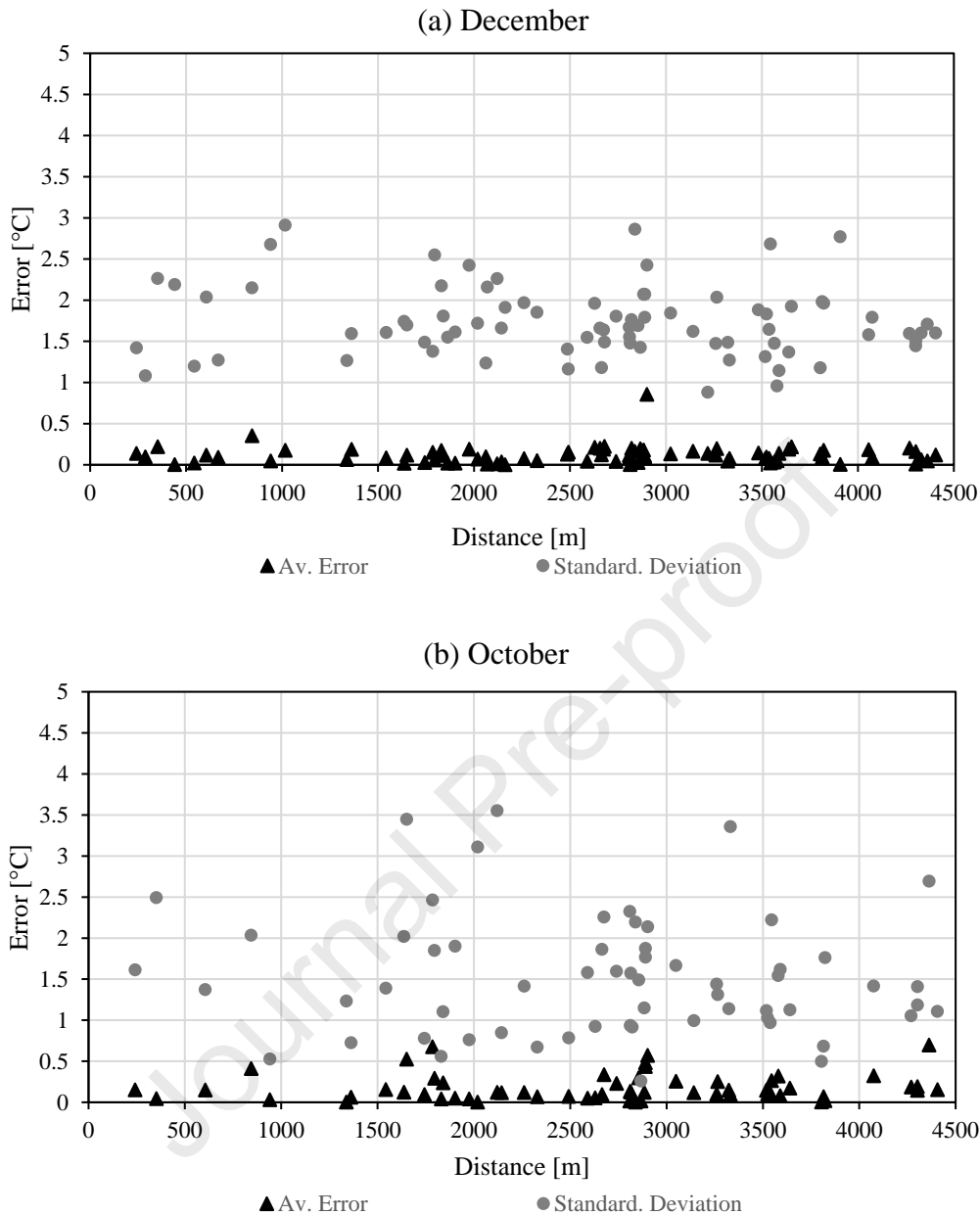
500

User	Distance [m]	<i>December</i>		<i>October</i>	
		Av. error [°C]	St. dev. [°C]	Av. error [°C]	St. dev. [°C]
<b>59</b>	4 405	0.12	1.60	-0.44	6.30
<b>64</b>	1 017	0.18	2.91	-0.05	3.46
<b>62</b>	2 811	0.09	1.55	0.39	4.62
<b>31</b>	4 302	0.16	1.51	0.06	5.71
<b>48</b>	941	0.05	2.68	-0.14	3.27
<b>38</b>	1 863	0.02	1.55	-1.33	5.51

Table 3.2 User supply temperature: average error and its standard deviation, root mean square error related to user location

501  
502 Table 3.2 summarizes the error in simulating the supply temperature for the selected users presented in the  
503 previous section. The same results but for the entire set of network's users are calculated and presented in a  
504 graphical form in Figure 3.12. It appears that neither the average errors neither its standard deviation increase  
505 with the distance from the generation plant. The average errors between monitored and simulated supply  
506 temperatures are due to incorrect estimation of the heat loss. There are many factors for this: the aging of the  
507 insulation which can vary the heat conductivity of pipes, non-uniform soil, the lack of insulation in some pipes  
508 or part of it, a certain inaccuracy in estimating the ground temperature. A deeper investigation on single aspects  
509 and components characteristics would reduce this error by better calibrating heat loss coefficients. The average  
510 errors do not measure the ability of the model to simulate temperature dynamics, which is instead evaluated  
511 by the standard deviation. Bigger errors can be noticed in October simulation. This can be explained by the  
512 monitoring data quality. In this period, heat demand and, consequently, flow rate are small, thus the  
513 measurements are affected by a larger uncertainty. The cause of bigger standard deviation errors can be the  
514 monitoring data logging time. In fact, in this period, frequent turning on and off can be noticed. Even if  
515 simulation time step is smaller, monitoring data are taken instantaneously every hour and linearly interpolated.  
516 This can cause an artificial time lag in the comparison of result. The level of accuracy of monitored data cannot  
517 give a sure explanation, these considerations remains possible reasons according to the authors. A more  
518 frequent and accurate monitoring system would be required to further analyse the cause of these errors.

519



520

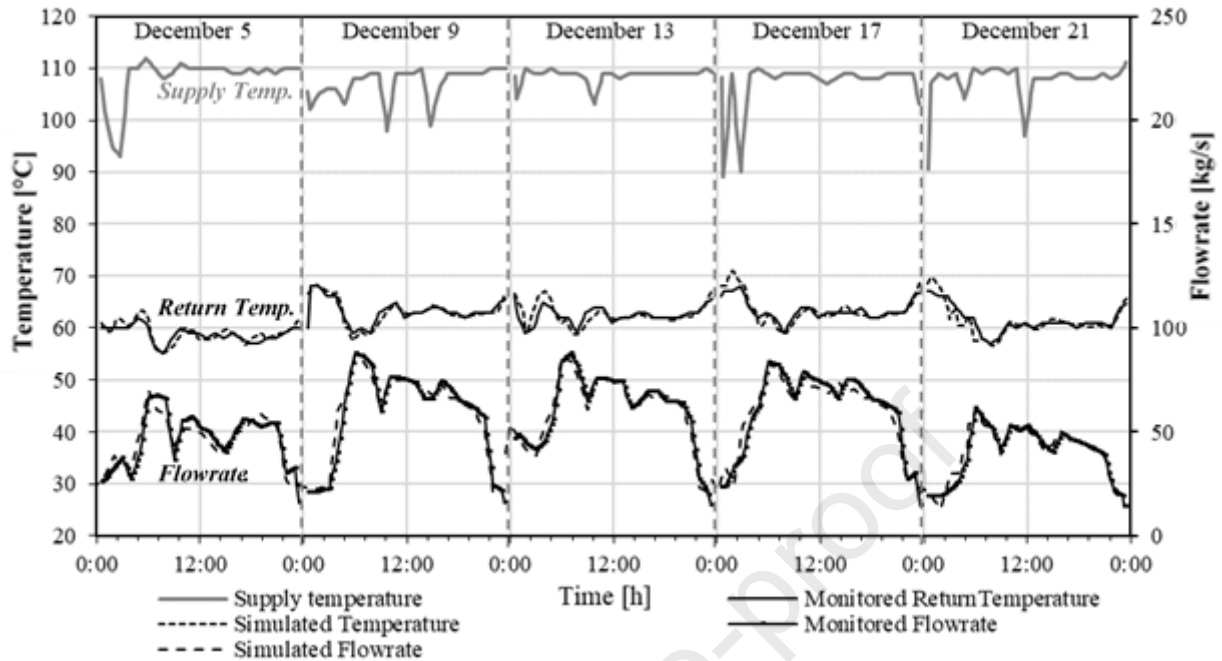
521

522

Figure 3.12 Correlation between supply temperature errors and user location in the network in December (a) and in October (b)

### 523 3.2.2 Return temperature and energy production of generation plant

524 The return temperature at generation plant predicted by simulation is presented in Figure 3.13, along with  
 525 temperature and flowrate monitored data. Five, non-consecutive, days have been analysed. The model output  
 526 profile is very close to the real one: the average error over the five days is  $-0.1\text{ }^{\circ}\text{C}$  while its standard deviation  
 527 is  $1.12\text{ }^{\circ}\text{C}$ .



528

529

Figure 3.13 Return temperature and flow rate at the generation plant – December

530

531

532

533

534

535

536

537

As for comparison at user's substations, the propagation time is satisfactorily simulated, especially considering that the monitoring data frequency is 1 hour. The morning peak demand, which here corresponds to the moments in which the return temperature has the minimum value, is the most critical day event for the generation plant: the model shows to predict it in an accurate way, considering both time correspondence and temperature values. The difference between predicted temperatures and the monitored ones is not uniform. The biggest discrepancies can be noticed in the very first hours of the day. In particular, on the 17<sup>th</sup> and the 21<sup>st</sup> of December, the simulated temperatures are higher than monitored ones; the lack of monitoring data in the previous time steps makes further investigations difficult.

538

539

540

Finally, the results of one-year simulation are presented in Table 3.3: the forecasted values come out being very close to energy production data given by the utility. Simulation time of the entire network composed by 485 edges is 2 hours and 7 minutes (Processor i-5 CPU 2.5GHz).

	Heat losses [MWh]	Heat production [MWh]
Simulation	5 710	36 642
Monitoring	5 832	36 769
Error	-2.1%	-0.3%

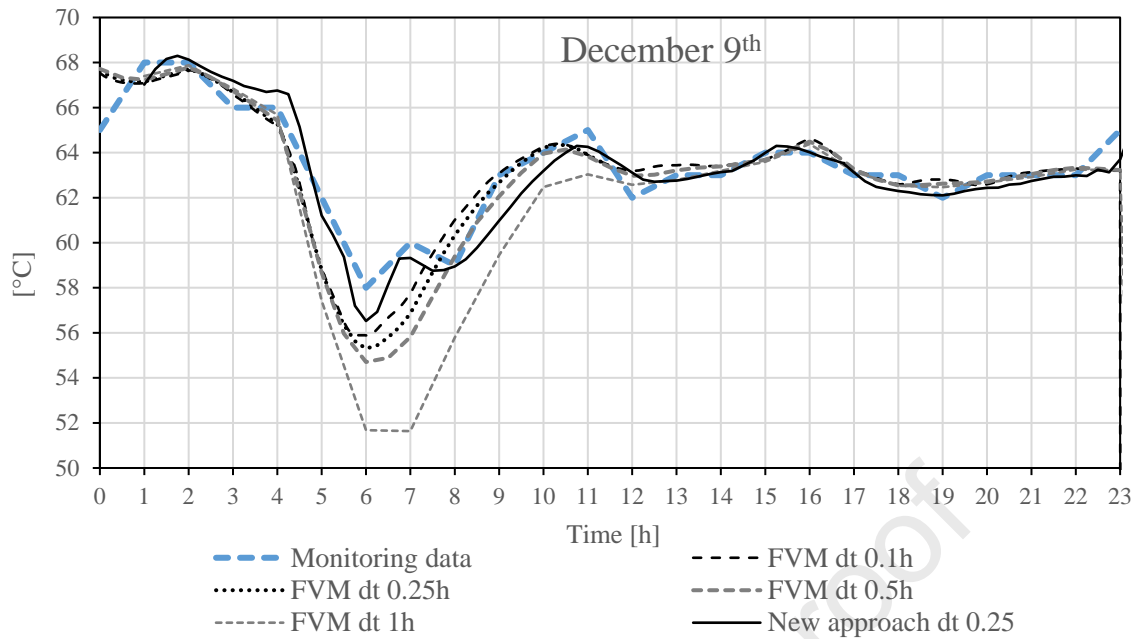
541

Table 3.3 Comparison between simulation and real measured heat losses and energy production at generation plant

542

543

Once the model is validated with monitoring data, it's worth comparing its performances with the other existing methods to see if all this work has been worth.



544

545

Figure 3.14 Return temperature at the generation plant FVM vs New approach simulation results –December 9<sup>th</sup>

546

547

548

549

550

551

552

Figure 3.14 shows the difference between the new model results and a finite volume method with lumped thermal capacity ( FVM with) different discretization mesh in time and space: the picture highlights the artificial diffusion which characterizes the discretization of FVM and it shows how the new approach produces results which are closer to monitoring data. Considering yearly energy results, the FVM with the same simulation time step,  $dt=0.25h$ , produces results with 3% and 0.5% errors respectively on heat losses and heat production, so generally bigger than the ones shown in Table 3.3. But most of all the difference lies in the inaccurate time delay which the FVM shows in Figure 3.14.

	Simulation	New method ( $dt=0.25h$ )	FVM ( $dt=0.25h$ )
Simulation time [s]	December 9 <sup>th</sup>	4.04 seconds	416 seconds
Standard deviation on return temperature [°C]	December 9 <sup>th</sup>	-0.3	-0.4
Average error on return temperature [°C]	December 9 <sup>th</sup>	0.6	1.5
Error on heat losses	Entire year	-2.1%	3%
Error on heat production	Entire year	-0.3%	5%

553

Table 3.4 Comparison between FVM and the developed method performances

554



## 555 **4 DISCUSSIONS AND CONCLUSIONS**

---

556 In this work the accuracy of a new modelling tool to simulate DH systems is investigated. The strength of the  
557 simulation tool lies in the flexibility of the modelling approach that can be chosen for each component in order  
558 to have better accuracy and lowest computational effort. The modularity of the model makes it suitable to  
559 simulate multicomponent systems such as city scale DH. The inclusion of the Lagrangian approach to model  
560 the network increases significantly the accuracy of the final results, avoiding the numerical diffusion effects  
561 still noticeable in existing models and reducing the simulation time. Nevertheless, the limit of this approach is  
562 that, in the current configuration, it can be used only for tree shaped network where the flow directions are  
563 known a-priori.

564 This work joins the list of few DH modelling tools that have been fully validated at system level with  
565 monitoring data. The monitoring data of a DH system in northern Italy have been used here to validate the  
566 presented model. The most important validation step is the comparison of its performances with real DH  
567 network monitoring data. This test is difficult to carry out because the quality of collected data in such a big  
568 and complex systems is often non satisfactory: monitoring data are often incomplete, monitoring devices are  
569 sometimes defective at user substations as well as at the generation plants or data logging works improperly.

570 A general problem is the inaccuracy of flow meters at very low loads which leads to bigger inaccuracies in  
571 mid-season and summer.

572 The validation of the model has been done accordingly to monitored data quality,: a certain degree of  
573 uncertainty still remains but the overall results are satisfactory. Especially results at distant points of the  
574 network show good correspondence to monitoring data and the model shows to properly forecast the peak in  
575 the central generation plant.

576 Looking at the validation outcomes, the model can be considered appropriate to make realistic assessments of  
577 the network behaviour in the presence of hypothetical structural changes, such as new branches or peripheral  
578 generators, in order to assess its economic convenience.

579 Considering its current use, for validation or network optimisation's purposes, the model needs to be fed by  
580 a significant quantity of monitoring input data in all users' substations, with all the problems previously  
581 mentioned.

582 A general problem of lack of good quality monitoring data in big systems is identified, especially for the  
583 hydraulic system behaviour. Nevertheless, dynamic simulation tools can be used exactly for this purpose so to  
584 predict the system's performances in all the points with no measurement devices.



585 Future development of the model includes the development of the Lagrangian approach for meshed networks  
586 and the estimation of user substations' behaviour in order to reduce the need of monitoring data.

587 **Acknowledgements**

588 The authors gratefully acknowledge Lodi Linea Green S.p.a. for providing monitoring data of the network.

589

Journal Pre-proof

590 **Appendix**

591 In this section the structure of the model describing the elements composing the network is described. The  
 592 different elements' models are defined as Types. The type model is composed by equations and parameters set  
 593 up functions grouped in cases which are called at every timestep.

594 **General structure of the type**

595 Case 1 – Initialisation of the variables

596 Case 2 – Inputs: read external files, parameters and previous steps results (+ calculation of substation flowrates  
 597 in user type)

598 Case 3 – Hydraulic problem: flowrates  $\dot{m}$ , pressures  $p$  and dissipation losses calculations  $\dot{Q}_{diss}$

599 Case 4 – Thermal problem: temperatures  $T$ , heat losses  $\dot{Q}_{loss}$ , internal energy change  $\Delta U$  calculations

600 Case 5 – Energy balance components (outputs): Work input and output, heat input and output, heat generation,  
 601 heat losses and internal energy change calculations

602 **Solution steps of the types**

603 Following the simulation steps of the model presented in Figure 2.4, here the functional programming approach  
 604 is described. For every step the suitable cases are recalled

Simulation step	Case	Types				Nodes
		Pipe	Pump	User	Generation	
Initialisation	1	$T_{in}, L$	$T_{in}$	$T_{in}$	$T_{in}$	$T_{nodes}$ - energy conservation
	2	$T_{ext}$		$\dot{Q}_{user}, \dot{m}_{user}$	$T_{gen}$	
Flowrates calculation	3	$\dot{m}$	$\dot{m}$		$\dot{m}$	Mass conservation
Pressures calculation	3	$p, \dot{Q}_{diss}$	$p, \dot{Q}_{diss}$	$p, \dot{Q}_{diss}$	$p, \dot{Q}_{diss}$	Momentum conservation
Temperatures calculations	4	$T, \dot{Q}_{loss}$	$T, \dot{Q}_{loss}, \Delta U$	$T, \dot{Q}_{loss}, \Delta U$	$T, \dot{Q}_{loss}, \Delta U$	
Outputs	5	$\dot{Q}_{loss}, \Delta U, \dot{Q}_{diss}$	$\dot{Q}_{loss}, \Delta U, \dot{Q}_{diss}, \dot{W}_{in}$	$\dot{Q}_{user}, \dot{Q}_{diss}$	$\dot{Q}_{gen}, \Delta U, \dot{W}_{in}$	

605 *Table 4.1 Simulation steps and relative cases and calculates state variables and outputs*

606

607 **Model equations of the types**608 **Pump**

$$\text{Hydraulic curve} \quad \Delta p = d \Delta p_{max} \left( 1 + k_1 \left| \frac{\dot{m}}{\dot{m}_{max}} \right| - (1 + k_1) \left| \frac{\dot{m}}{\dot{m}_{max}} \right|^2 \right)$$

$$\text{Momentum} \quad p_{out} - p_{in} = \Delta p - a L |\dot{m}| \dot{m}$$

$$\text{Efficiency curve} \quad \eta = e_0 + e_1 \left( \frac{\dot{m}}{\dot{m}_{max}} \right) + e_2 \left( \frac{\dot{m}}{\dot{m}_{max}} \right)^2$$

$$\text{Heat dissipation} \quad \dot{Q}_{diss} = \frac{\dot{m}}{\rho} \left( |\Delta p| \left( \frac{1}{\eta} - 1 \right) + a L \dot{m}^2 \right)$$

$$\text{Power consumption} \quad W = \frac{\frac{\dot{m}}{\rho} |\Delta p|}{\eta}$$

$$\text{Heat loss} \quad \dot{Q}_{loss} = UA L (T - T_{ext})$$

- 609 •  $d$  pump direction, 1 if from node(in) to node(out), -1 if from node(out) to node(in)
- 610 •  $\Delta p_{max}$  hydraulic head with zero mass flow rate
- 611 •  $\dot{m}_{max}$  mass flow rate with zero hydraulic head
- 612 •  $k_1$  first-order coefficient of the normalized hydraulic curve
- 613 •  $e_0$  zero-order coefficient of the efficiency curve
- 614 •  $e_1$  first-order coefficient of the efficiency curve
- 615 •  $e_2$  second-order coefficient of the efficiency curve
- 616 •  $a$  quadratic pressure drop coefficient per unit length
- 617 •  $UA$  UA value of pipe per unit length
- 618 •  $L$  element length
- 619 •  $T_{ext}$  external temperature

620 **Pipe**

$$\text{Momentum} \quad p_{out} - p_{in} = \Delta p - a L |\dot{m}| \dot{m}$$

$$\text{Heat dissipation} \quad \dot{Q}_{diss} = \frac{\dot{m}}{\rho} \left( |\Delta p| \left( \frac{1}{\eta} - 1 \right) + a L \dot{m}^2 \right)$$

$$\text{Heat loss} \quad \dot{Q}_{loss} = UA L (T - T_{ext})$$

- 621 •  $a$  quadratic pressure drop coefficient per unit length
- 622 •  $UA$  UA value of pipe per unit length
- 623 •  $L$  element length
- 624 •  $T_{ext}$  external temperature

625

626 **Substation (with assigned thermal load and secondary circuit temperatures)**

Heat dissipation  $\dot{Q}_{diss} = \frac{\dot{m}}{\rho} \left( |\Delta p| \left( \frac{1}{\eta} - 1 \right) + aL\dot{m}^2 \right)$

Return temperature  $\frac{[(T_{s1} - T_{s2}) - (T_{r1} - T_{r2})]}{\ln\left(\frac{T_{s1} - T_{s2}}{T_{r1} - T_{r2}}\right)} = \frac{\dot{Q}_{user}}{UA_{HX}}$

Flowrate  $\dot{m} = \min\left(\dot{m}_{max}, \frac{\dot{Q}_{user}}{[c_p(T_{s1} - T_{r1})]}\right)$

- 627 •  $\dot{Q}_{user}$  thermal load (positive for heating)
- 628 •  $L$  element length
- 629 •  $UA_{HX}$  heat exchanger UA value
- 630 •  $T_{ext}$  external temperature
- 631 •  $T_{s1}, T_{r1}$  supply and return temperature on the primary side of the heat exchanger
- 632 •  $T_{s2}, T_{r2}$  supply and return temperature on the secondary side of the heat exchanger
- 633 •  $\dot{m}_{max}$  maximum (design) mass flow rate

634 **Generator with constant outlet temperature**

Momentum  $p_{out} - p_{in} = \Delta p - aL|\dot{m}|\dot{m}$

Heat dissipation  $\dot{Q}_{diss} = \frac{\dot{m}}{\rho} \left( |\Delta p| \left( \frac{1}{\eta} - 1 \right) + aL\dot{m}^2 \right)$

Heat generation  $\dot{Q}_{gen} = |\dot{m}|c_p(T_{set} - T_{in}) - \dot{Q}_{diss}$

- 635 •  $a$  quadratic pressure drop coefficient per unit length
- 636 •  $L$  element length
- 637 •  $T_{set}$  outlet temperature set point

638

639 **References**

- 640 [1] European Union, Directive 2012/27/EU on energy efficiency, 2012.
- 641 [2] European Commission, Communication COM(2016) 51 final. An EU Strategy on Heating and Cooling,  
642 2016.
- 643 [3] L. Brange, J. Englund, P. Lauenburg, Prosumers in district heating networks - A Swedish case study,  
644 *Appl. Energy*. 164 (2016) 492–500. doi:10.1016/j.apenergy.2015.12.020.
- 645 [4] P.M.Á. De Urbarri, U. Eicker, D. Robinson, Energy performance of decentralized solar thermal feed-  
646 in to district heating networks, in: *Energy Procedia*, 2017: pp. 285–296.  
647 doi:10.1016/j.egypro.2017.05.075.
- 648 [5] B. Di Pietra, F. Zanghirella, G. Puglisi, An evaluation of distributed solar thermal “net metering” in  
649 small-scale district heating systems, in: *Energy Procedia*, 2015: pp. 1859–1864.  
650 doi:10.1016/j.egypro.2015.11.335.
- 651 [6] L. Brand, A. Calvén, J. Englund, H. Landersjö, P. Lauenburg, Smart district heating networks - A  
652 simulation study of prosumers’ impact on technical parameters in distribution networks, *Appl. Energy*.  
653 129 (2014) 39–48. doi:10.1016/j.apenergy.2014.04.079.
- 654 [7] S. Buffa, M. Cozzini, M. D’Antoni, M. Baratieri, R. Fedrizzi, 5th generation district heating and cooling  
655 systems: A review of existing cases in Europe, *Renew. Sustain. Energy Rev.* 104 (2019) 504–522.  
656 doi:10.1016/j.rser.2018.12.059.
- 657 [8] H. Lund, N. Duic, P.A. Østergaard, B.V. Mathiesen, Future district heating systems and technologies:  
658 On the role of smart energy systems and 4th generation district heating, *Energy*. 165 (2018) 614–619.  
659 doi:10.1016/j.energy.2018.09.115.
- 660 [9] H. Lund, P.A. Østergaard, T.B. Nielsen, S. Werner, J.E. Thorsen, O. Gudmundsson, A. Arabkoohsar,  
661 B.V. Mathiesen, Perspectives on fourth and fifth generation district heating, *Energy*. 227 (2021)  
662 120520. doi:10.1016/j.energy.2021.120520.
- 663 [10] A. Dénarié, M. Aprile, M. Motta, Heat transmission over long pipes: New model for fast and accurate  
664 district heating simulations, *Energy*. 166 (2019) 267–276. doi:10.1016/J.ENERGY.2018.09.186.
- 665 [11] A. Benonysson, Dynamic modelling and operation optimization of district heating systems, PhD  
666 Thesis, Technical University of Denmark (DTU), Denmark, 1991.
- 667 [12] J. Dancker, M. Wolter, Improved quasi-steady-state power flow calculation for district heating systems:  
668 A coupled Newton-Raphson approach, *Appl. Energy*. 295 (2021) 116930.

- 669 doi:10.1016/j.apenergy.2021.116930.
- 670 [13] V.D. Stevanovic, S. Prica, B. Maslovaric, B. Zivkovic, S. Nikodijevic, Efficient numerical method for  
671 district heating system hydraulics, *Energy Convers. Manag.* 48 (2007) 1536–1543.  
672 doi:10.1016/j.enconman.2006.11.018.
- 673 [14] Y. Wang, X. Wang, L. Zheng, X. Gao, Z. Wang, S. You, H. Zhang, S. Wei, Thermo-hydraulic coupled  
674 analysis of long-distance district heating systems based on a fully-dynamic model, *Appl. Therm. Eng.*  
675 222 (2023) 119912. doi:10.1016/j.applthermaleng.2022.119912.
- 676 [15] I. Ben Hassine, U. Eicker, Impact of load structure variation and solar thermal energy integration on an  
677 existing district heating network, *Appl. Therm. Eng.* 50 (2013) 1437–1446.  
678 doi:10.1016/j.applthermaleng.2011.12.037.
- 679 [16] E. Guelpa, A. Sciacovelli, V. Verda, Thermo-fluid dynamic model of large district heating networks  
680 for the analysis of primary energy savings, *Energy*. 184 (2019) 34–44.  
681 doi:10.1016/j.energy.2017.07.177.
- 682 [17] J. Vivian, D. Quaggiotto, A. Zarrella, Increasing the energy flexibility of existing district heating  
683 networks through flow rate variations, *Appl. Energy*. 275 (2020) 115411.  
684 doi:10.1016/j.apenergy.2020.115411.
- 685 [18] M. Vesterlund, J. Dahl, A method for the simulation and optimization of district heating systems with  
686 meshed networks, *Energy Convers. Manag.* 89 (2015) 555–567. doi:10.1016/j.enconman.2014.10.002.
- 687 [19] K. Sartor, D. Thomas, P. Dewallef, A comparative study for simulating heat transport in large district  
688 heating networks, in: *ECOS 2015 Int. Conf.*, Pau, France, 2015.
- 689 [20] H. V Larsen, B. Bøhm, M. Wigbels, A comparison of aggregated models for simulation and operational  
690 optimisation of district heating networks, *Energy Convers. Manag.* 45 (2004) 1119–1139.  
691 doi:10.1016/j.enconman.2003.08.006.
- 692 [21] H. Pálsson, *Methods for planning and operating decentralised combined heat and power plants*, PhD  
693 Thesis, Riso National Laboratory, Roskilde, Denmark, 2000.
- 694 [22] A. Dalla Rosa, H. Li, S. Svendsen, Method for optimal design of pipes for low-energy district heating,  
695 with focus on heat losses, *Energy*. 36 (2011) 2407–2418. doi:10.1016/j.energy.2011.01.024.
- 696 [23] A. Dalla Rosa, H. Li, S. Svendsen, Modeling Transient Heat Transfer in Small-Size Twin Pipes for  
697 End-User Connections to Low- Energy District Heating Networks, *Heat Transf. Eng.* ISSN. 34 (2013)

- 698 372–384. doi:10.1080/01457632.2013.717048.
- 699 [24] I. Gabrielaitiene, B. Bøhm, B. Sunden, Evaluation of Approaches for Modeling Temperature Wave  
700 Propagation in District Heating Pipelines, *Heat Transf. Eng.* 29 (2008) 45–56.  
701 doi:10.1080/01457630701677130.
- 702 [25] I. Gabrielaitiene, Numerical Simulation of a District Heating System with Emphases on Transient  
703 Temperature Behaviour, in: 8th Int. Conf. Environ. Eng., Vilnius, 2011: pp. 747–754.
- 704 [26] I. Gabrielaitienė, B. Bøhm, B. Sundén, Dynamic temperature simulation in district heating systems in  
705 Denmark regarding pronounced transient behaviour, *J. Civ. Eng. Manag.* 17 (2011) 79–87.  
706 doi:10.3846/13923730.2011.553936.
- 707 [27] I. Gabrielaitiene, B. Sunden, B. Bøhm, H. Larsen, Dynamic performance of district heating system in  
708 Madumvej, Denmark, in: 10th Int. Symp. Dist. Heat. Cool., Hanover, 2006.
- 709 [28] I. Gabrielaitiene, B. Bøhm, B. Sunden, Modelling temperature dynamics of a district heating system in  
710 Naestved, Denmark—A case study, *Energy Convers. Manag.* 48 (2007) 78–86.  
711 doi:10.1016/j.enconman.2006.05.011.
- 712 [29] S.E.L.U. of Wisconsin-Madison, TRNSYS 16 Mathematical Reference, 2006. doi:10.1108/978-1-  
713 78743-527-820181015.
- 714 [30] T. Oppelt, T. Urbaneck, U. Gross, B. Platzer, Dynamic thermo-hydraulic model of district cooling  
715 networks, *Appl. Therm. Eng.* (2016). doi:10.1016/j.applthermaleng.2016.03.168.
- 716 [31] J. Maurer, O.M. Ratzel, A.J. Malan, S. Hohmann, Comparison of discrete dynamic pipeline models for  
717 operational optimization of District Heating Networks, *Energy Reports.* 7 (2021) 244–253.  
718 doi:10.1016/j.egy.2021.08.150.
- 719 [32] S.S. Meibodi, S. Rees, Dynamic thermal response modelling of turbulent fluid flow through pipelines  
720 with heat losses, *Int. J. Heat Mass Transf.* 151 (2020) 119440.  
721 doi:10.1016/j.ijheatmasstransfer.2020.119440.
- 722 [33] G. Barone, A. Buonomano, C. Forzano, A. Palombo, A novel dynamic simulation model for the  
723 thermo-economic analysis and optimisation of district heating systems, *Energy Convers. Manag.* 220  
724 (2020) 113052. doi:10.1016/j.enconman.2020.113052.
- 725 [34] J. Steinegger, S. Wallner, M. Greiml, T. Kienberger, A new quasi-dynamic load flow calculation for  
726 district heating networks, *Energy.* 266 (2023) 126410. doi:10.1016/j.energy.2022.126410.
- 727 [35] L. Giraud, R. Baviere, M. Vallée, C. Paulus, Presentation, Validation and Application of the District

- 728 Heating Modelica Library, Proc. 11th Model. Conf. (2015) 79–88. doi:10.3384/ecp1511879.
- 729 [36] B. Van Der Heijde, M. Fuchs, C.R. Tugores, G. Schweiger, K. Sartor, D. Basciotti, D. Müller, C.  
730 Nytsch-Geusen, M. Wetter, L. Helsen, Dynamic equation-based thermo-hydraulic pipe model for  
731 district heating and cooling systems, *Energy Convers. Manag.* 151 (2017) 158–169.  
732 doi:10.1016/j.enconman.2017.08.072.
- 733 [37] Python, (n.d.). <https://www.python.org/>.
- 734 [38] J. Röder, B. Meyer, U. Krien, J. Zimmermann, T. Stührmann, E. Zondervan, Optimal design of district  
735 heating networks with distributed thermal energy storages – method and case study, *Int. J. Sustain.*  
736 *Energy Plan. Manag.* 31 (2021) 5–22. doi:10.5278/ijsepm.6248.
- 737 [39] oemof community, DHNx, (n.d.). <https://github.com/oemof/DHNx>.
- 738 [40] oemof community, Oemof, (n.d.). <https://github.com/oemof/>.
- 739 [41] L. Vorspel, J. Bücker, District-heating-grid simulation in python: Digripy, *Computation.* 9 (2021).  
740 doi:10.3390/computation9060072.
- 741 [42] F. Witte, I. Tuschy, TESPpy: Thermal Engineering Systems in Python, *J. Open Source Softw.* 5 (2020)  
742 2178. doi:10.21105/joss.02178.
- 743 [43] K. Sartor, P. Dewalef, Experimental validation of heat transport modelling in district heating networks,  
744 *Energy.* 137 (2017) 961–968. doi:10.1016/j.energy.2017.02.161.
- 745 [44] D.C. Kozen, Depth-First and Breadth-First Search, in: *Des. Anal. Algorithms. Texts Monogr. Comput.*  
746 *Sci.*, Springer, New York, NY, 1992: pp. 19–24. doi:10.1007/978-1-4612-4400-4\_4.
- 747 [45] P.D. Lax, *Hyperbolic Systems of Conservation Laws and the Mathematical Theory of Shock Waves*,  
748 Society for Industrial and Applied Mathematics, 1973. doi:doi:10.1137/1.9781611970562.ch1.
- 749 [46] J.H. Lienhard, IV, J.H. Lienhard, V, *A Heat Transfer Textbook*, Fourth Ed., Phlogiston Press,  
750 Cambridge, MA, 2017.
- 751 [47] F.E. Toro, *Riemann Solvers and Numerical Methods for Fluid Dynamics*, Springer, Berlin, Heidelberg,  
752 1999.
- 753 [48] AIRU, *Il riscaldamento urbano - Annuario 2013*, Tecnedi, Milano, 2013.

754



**Declaration of interests**

The authors declare that they have no known competing financial interests or personal relationships that could have appeared to influence the work reported in this paper.

The authors declare the following financial interests/personal relationships which may be considered as potential competing interests:

Journal Pre-proof